Electronic Supplementary Material (ESI) for Green Chemistry.

Supplementary Information

Design of supported organocatalysts from a biomass-derived difuran compound and catalytic assessment for lactose hydrolysis

Hochan Chang[a], Alexios G. Stamoulis[b], George W. Huber[a], and James A. Dumesic[a,c]*

[a]Department of Chemical and Biological Engineering, University of Wisconsin–Madison, Madison, WI, USA.

[b]Department of Chemistry, University of Wisconsin–Madison, Madison, WI, USA.

[c]DOE Great Lakes Bioenergy Research Center, University of Wisconsin–Madison, 1552 University Avenue, Madison, WI, USA.

*Corresponding author E-mail: jdumesic@wisc.edu

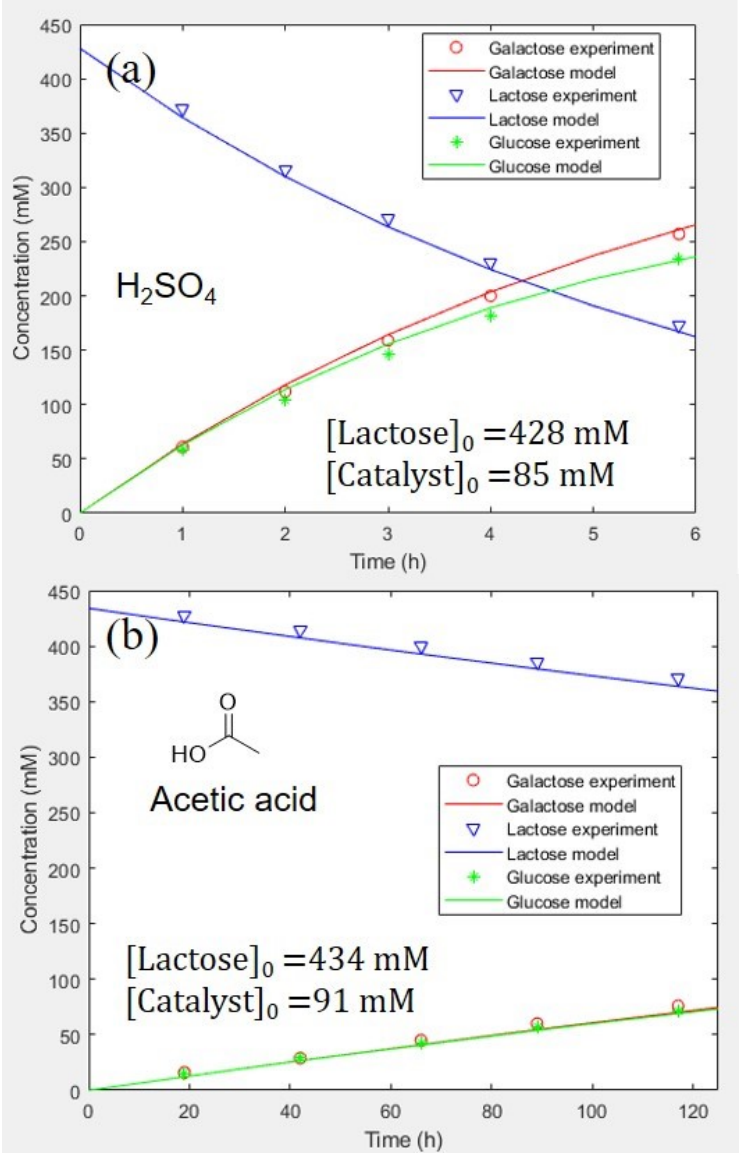

Figure S1. Reaction kinetics analysis for lactose hydrolysis (at 100°C) in presence of (a) sulfuric acid (k_{app}=0.1615 ± 0.0075 h^{-1}, $k_{d,app}$=0.0039 ± 0.0195 h^{-1}) and (b) acetic acid (k_{app}=0.0015 ± 0.0001 h^{-1}, $k_{d,app}$=0.0003 ± 0.0015 h^{-1}) for the calculation of rate constants for H^+ (k_{H+}) and non-dissociated acetic acid (k_{AA}). k_{app} and $k_{d,app}$ represent the apparent rate constants for lactose hydrolysis and glucose degradation, respectively and the values are evaluated within 95% confidential intervals; Rate = $k_{app}\cdot[\text{Lactose}]_0$ = $k_{H+}\cdot[H^+]\cdot[\text{Lactose}]_0$ for sulfuric acid and Rate = $k_{app}\cdot[\text{Lactose}]_0 = (k_{H+}\cdot[H^+] + k_{AA}\cdot[\text{AA}])\cdot[\text{Lactose}]_0$ (AA represents acetic acid).

$$\begin{cases} OAc^- + H^+ \rightleftharpoons HOAc, K_1 = 1/K_{HOAc} \\ G_1H \rightleftharpoons G_1 + H^+, K_2 = K_{G_1H} \\ G_2H \rightleftharpoons G_2 + H^+, K_3 = K_{G_2H} \\ G_N + H^+ \rightleftharpoons G_NH, K_4 = 1/K_{G_NH} \end{cases}$$

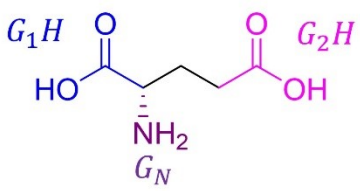

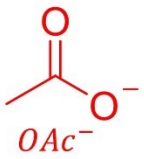

$$\begin{cases} K_1 = \dfrac{x}{([OAc^-]_0 - x) \cdot [H^+]} & \text{pK}_a = 4.76 \\ K_2 = \dfrac{y \cdot [H^+]}{[G_1H]_0 - y} & \text{pK}_a = 2.19 \\ K_3 = \dfrac{z \cdot [H^+]}{[G_2H]_0 - z} & \text{pK}_a = 4.25 \\ K_4 = \dfrac{m}{([G_N]_0 - m) \cdot [H^+]} & \text{pK}_a = 9.67 \end{cases}$$

$$[H^+] = [H^+]_0 - x + y + z - m$$

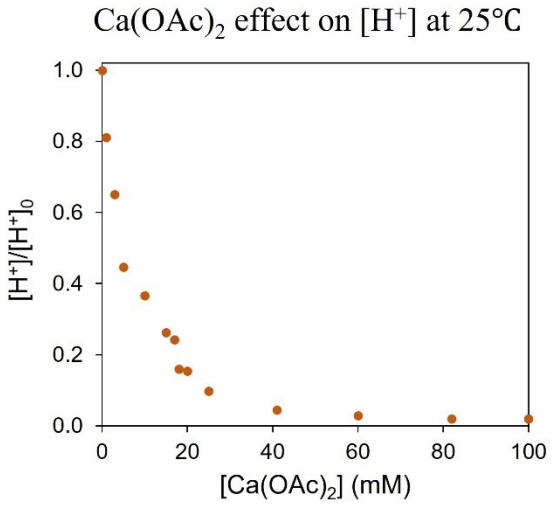

Figure S2. Theoretical derivation of $Ca(OAc)_2$ effect on the $[H^+]$ in glutamic acid solution with $Ca(OAc)_2$ and the normalized $[H^+]$ ($[H^+]/[H^+]_0$) profile at 25°C by the theoretical calculation ($[H^+]_0$ represents $[H^+]$ in glutamic acid solution without $Ca(OAc)_2$).

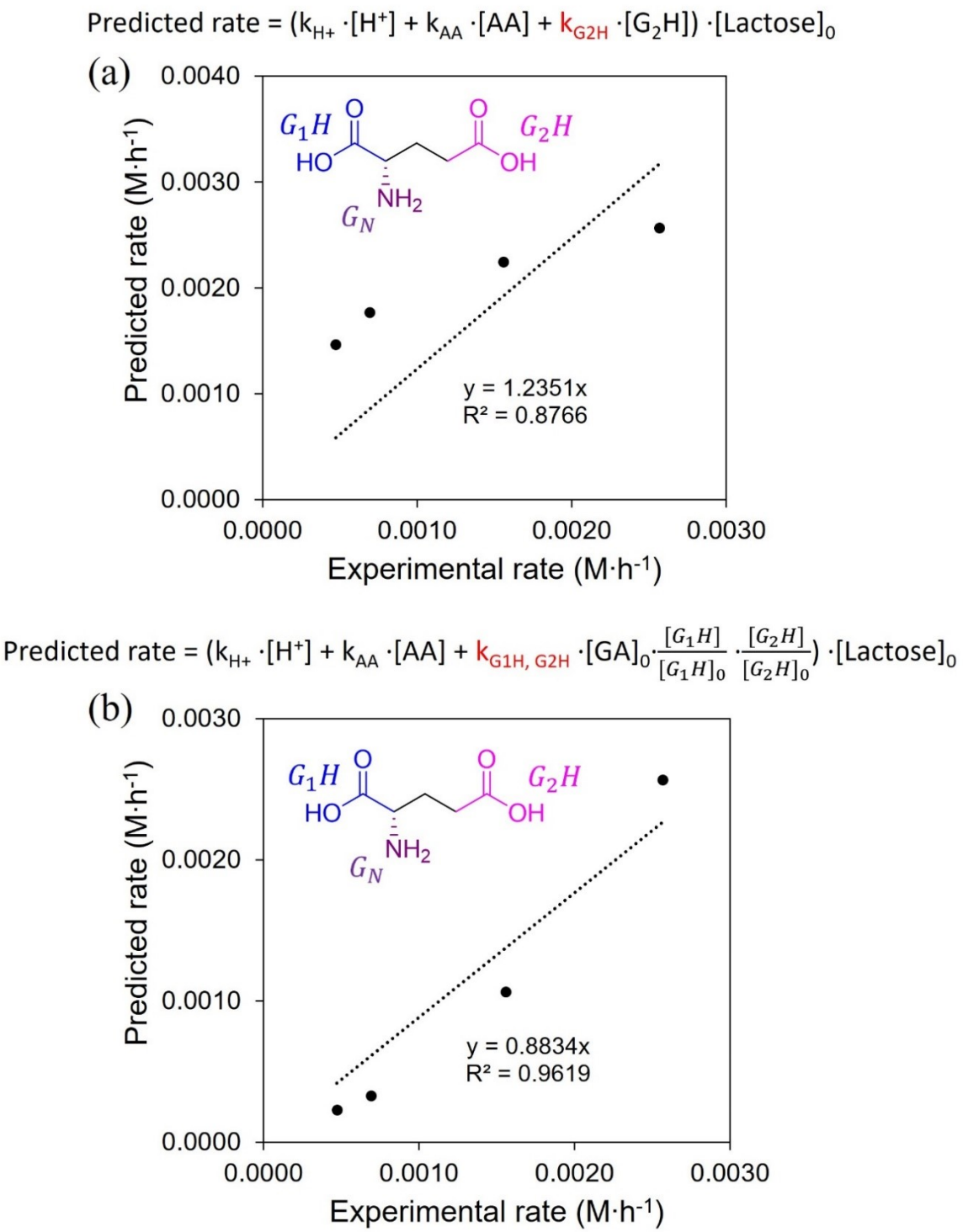

Figure S3. Active site analysis in glutamic acid by model fitting for theoretical and experimental reaction rate for lactose hydrolysis in the presence of $Ca(OAc)_2$. The active site was assumed as (a) a single active site of G_2H and (b) dual active sites of G_1H and G_2H (k_{H+}, k_{G2H}, and $k_{G1H,G2H}$ represent the rate constant from H^+, G_2H, and combination of G_1H and G_2H as an active site in glutamic acid moiety, respectively).

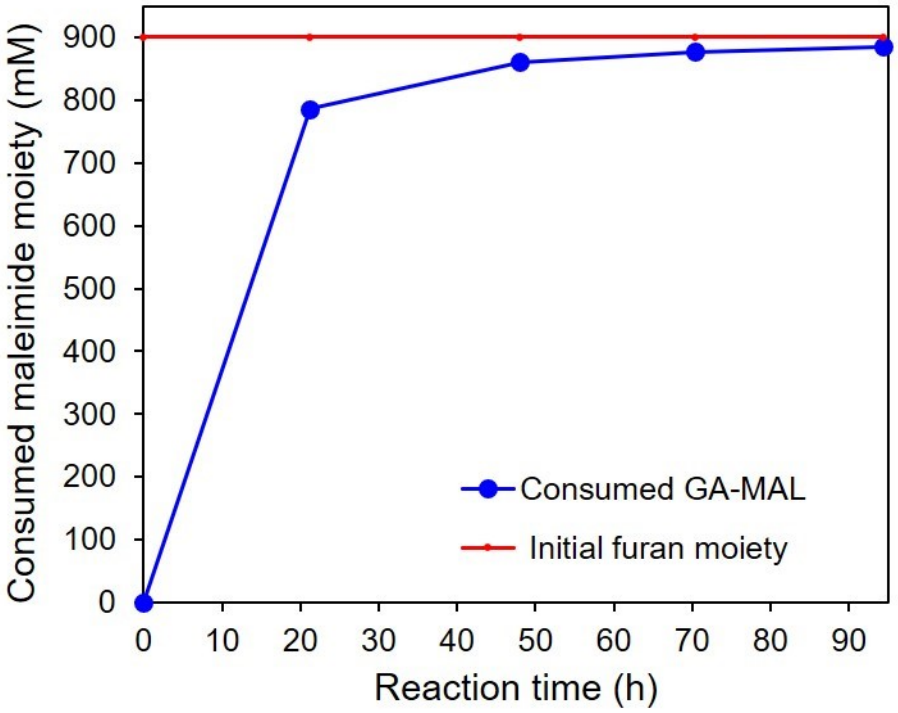

Figure S4. Conversion of GA-MAL by Diels-Alder reaction with PHAH over the reaction time (measured by HPLC).

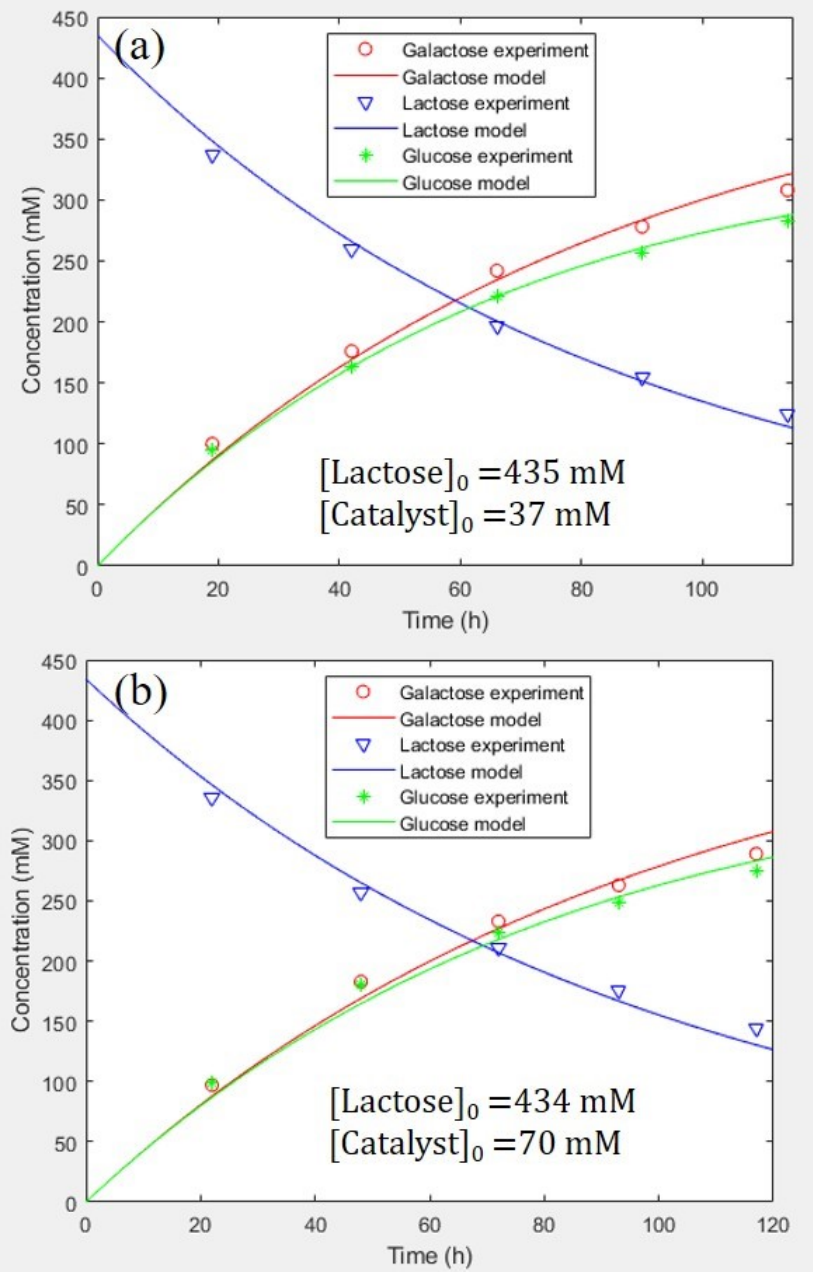

Figure S5. Reaction kinetics analysis for lactose hydrolysis (at 100°C) in presence of (a) 37 mM (k_{app}=0.0117 ± 0.0004 h^{-1}, $k_{d,app}$=0.0016 ± 0.0005 h^{-1}) and (b) 70 mM (k_{app}=0.0103 ± 0.0004 h^{-1}, $k_{d,app}$=0.0010 ± 0.0006 h^{-1}) of homogeneous PHAH-GA-MAL-H. (k_{app}: apparent rate constants for lactose hydrolysis, $k_{d,app}$: apparent rate constant for glucose degradation within 95% confidential intervals).

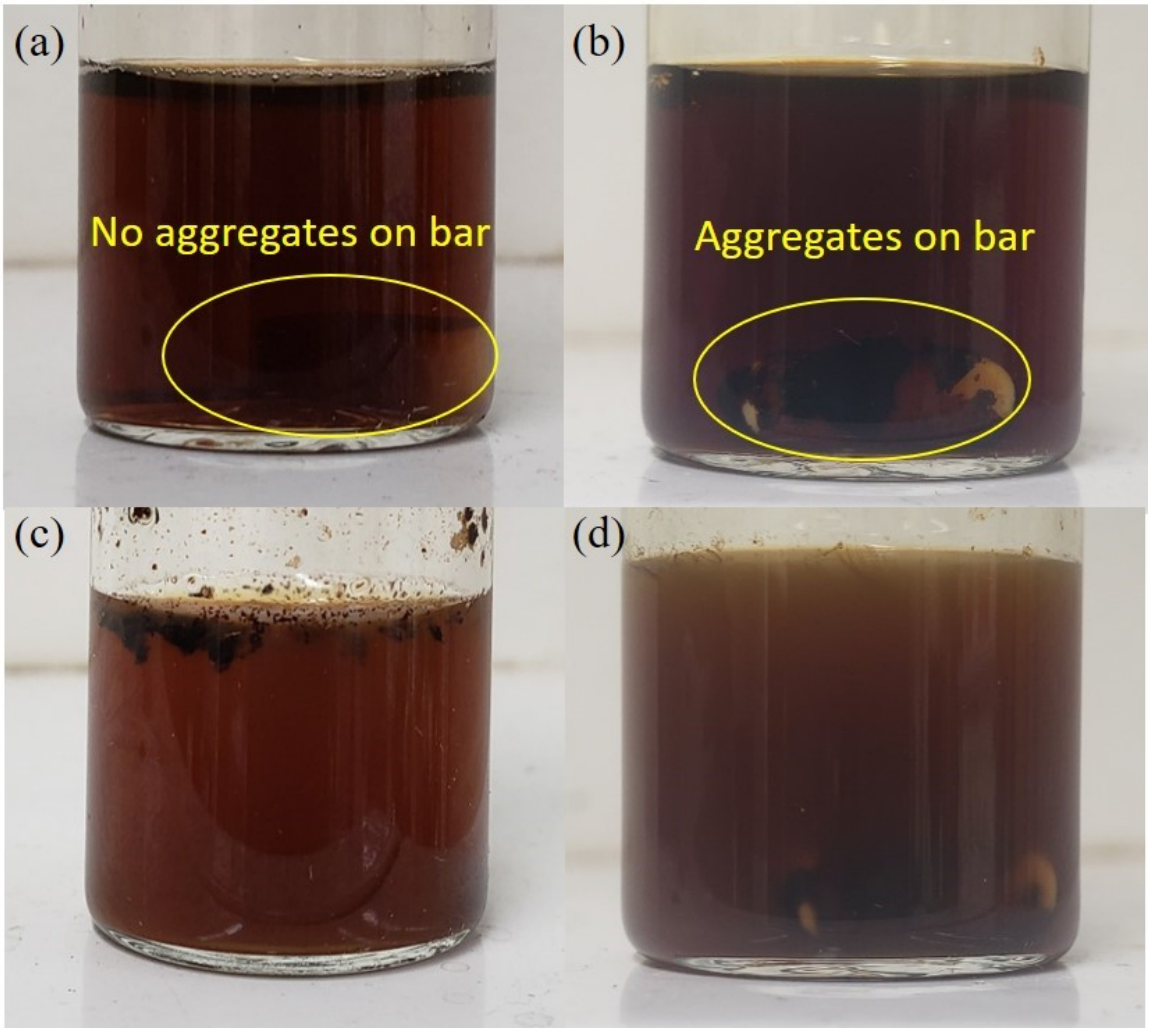

Figure S6. Images of PHAH-GA-MAL-H solution in water at different temperature. Concentration of PHAH-GA-MAL-H is (a) 37 mM (=27.04 g/L) at 100°C, (b) 70 mM (=51.16 g/L) at 100°C, (c) 37 mM at room temperature, and (d) 70 mM at room temperature.

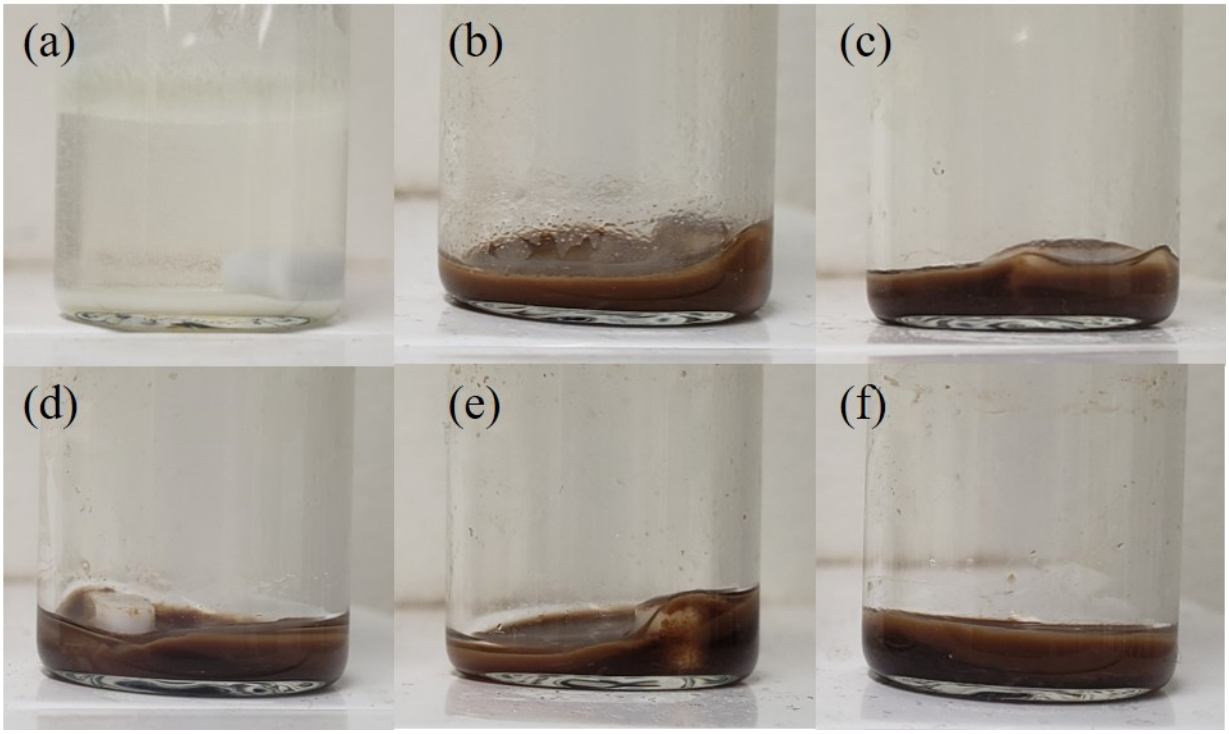

Figure S7. Images of (a) the fresh immobilized catalyst (white solid at the bottom of vial, 16wt% loading of PHAH-GA-MAL on Si-C_4) in feed solution and the used catalyst after (b) 1st, (c) 2nd, (d) 3rd, (e) 4th, and (f) 5nd cycle of lactose hydrolysis (brown solid at the bottom of vial, at 100°C).

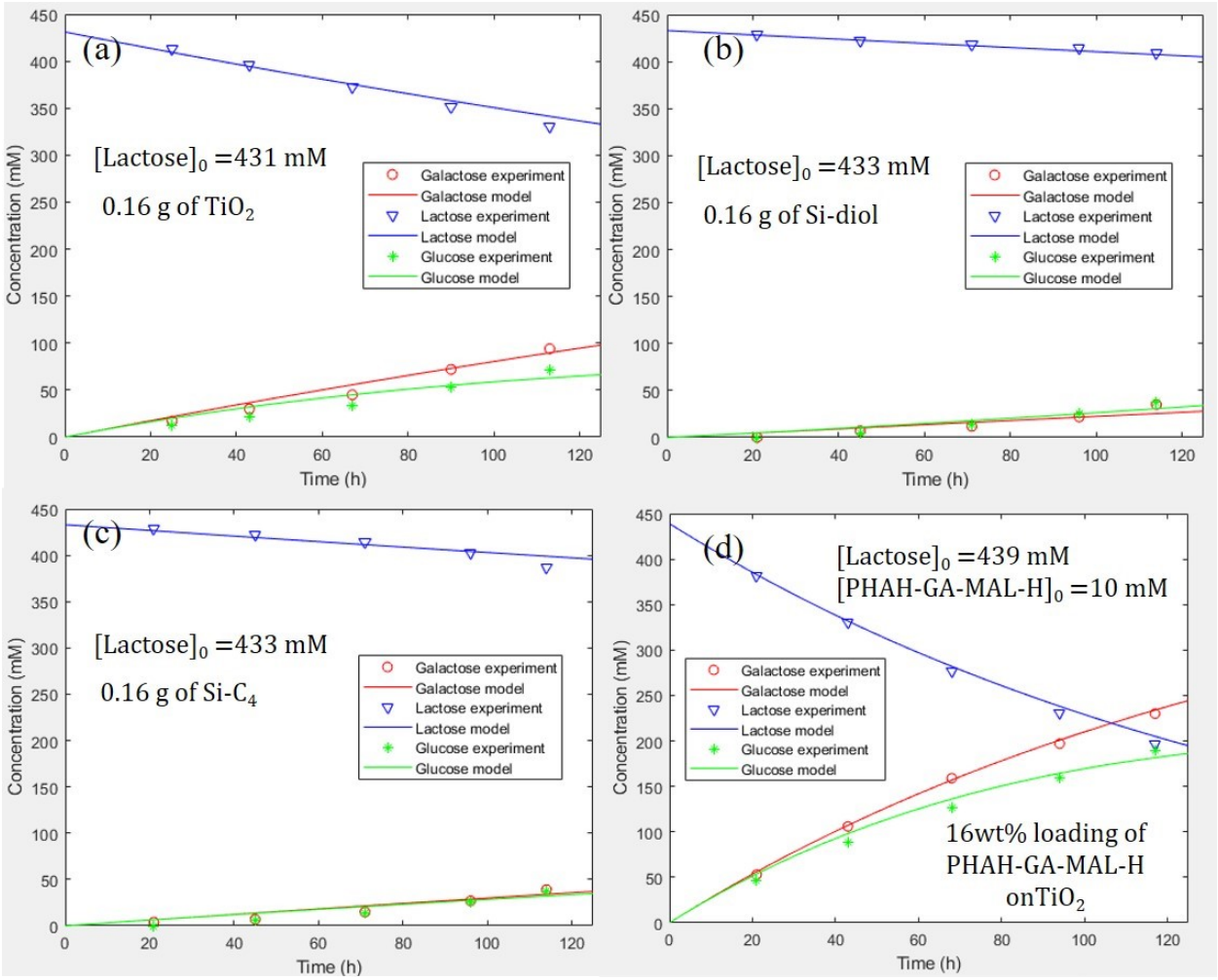

Figure S8. Reaction kinetics analysis for lactose hydrolysis (at 100°C) over the (a) TiO_2 (k_{app}=0.0021 ± 0.0001 h^{-1}, $k_{d,app}$=0.0064 ± 0.0023 h^{-1}), (b) Si-diol (k_{app}=0.0005 ± 0.0001 h^{-1}, $k_{d,app}$=-0.0031 ± 0.0029 h^{-1}), (c) Si-C_4 (k_{app}=0.0007 ± 0.0001 h^{-1}, $k_{d,app}$=0.0010 ± 0.0035 h^{-1}) (0.16 g of bare support), and (d) PHAH-GA-MAL-H (16wt% loading) on TiO_2 (k_{app}=0.0065 ± 0.0002 h^{-1}, $k_{d,app}$=0.0040 ± 0.0007 h^{-1}); (k_{app}: apparent rate constants for lactose hydrolysis, $k_{d,app}$: apparent rate constant for glucose degradation within 95% confidential intervals).

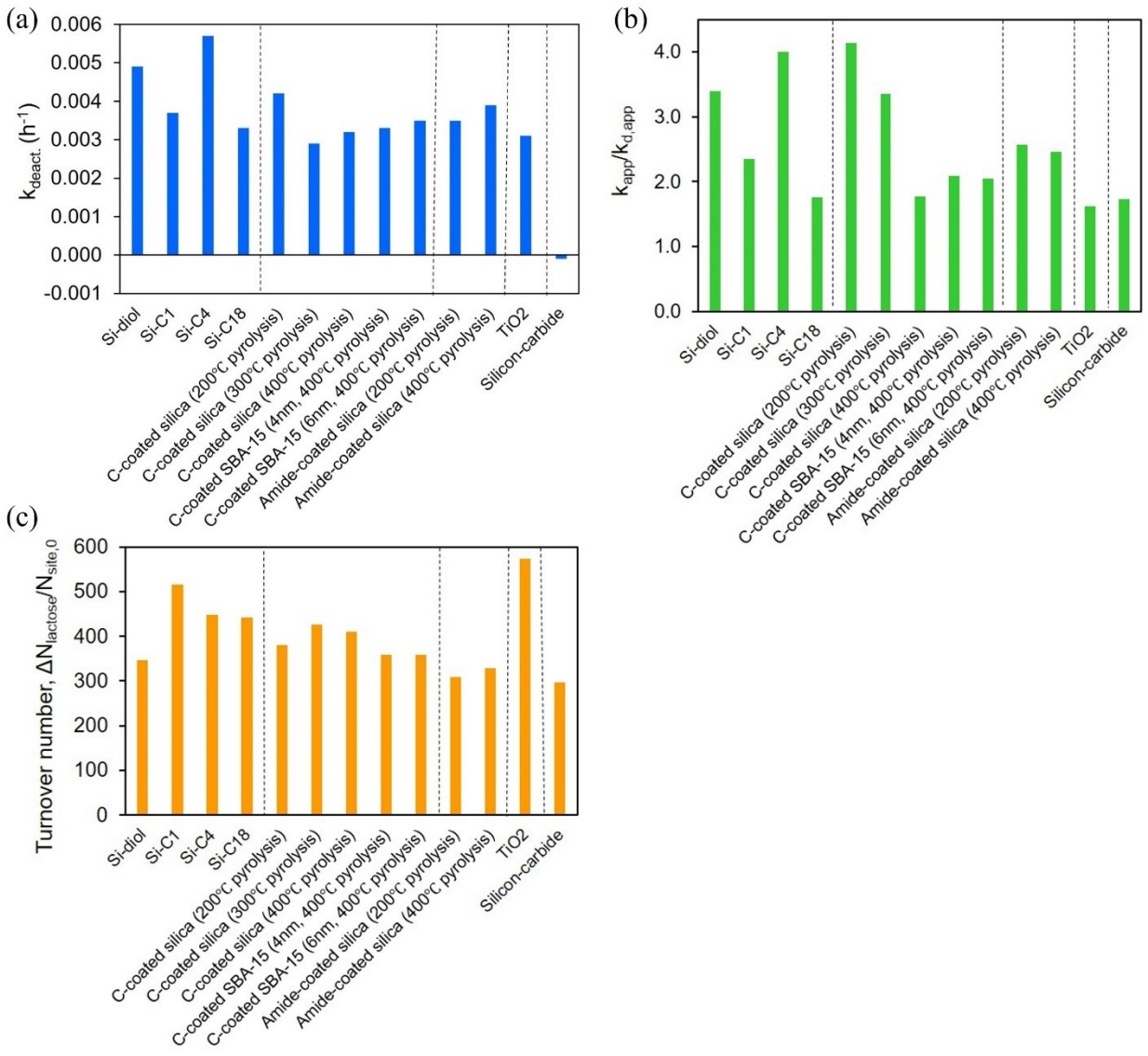

Figure S9. Effect of various supports on (a) catalyst stability, (b) catalyst selectivity, and (c) total turnover numbers (16 wt% loading of PHAH-GA-MAL-H on supports) for lactose hydrolysis. Reaction conditions: 420-435 mM of aqueous lactose solution was hydrolyzed at 100℃ in the presence of various catalysts; Rate for each hydrolysis cycle were measured by reaction kinetics analysis for 110-120 h of hydrolysis.

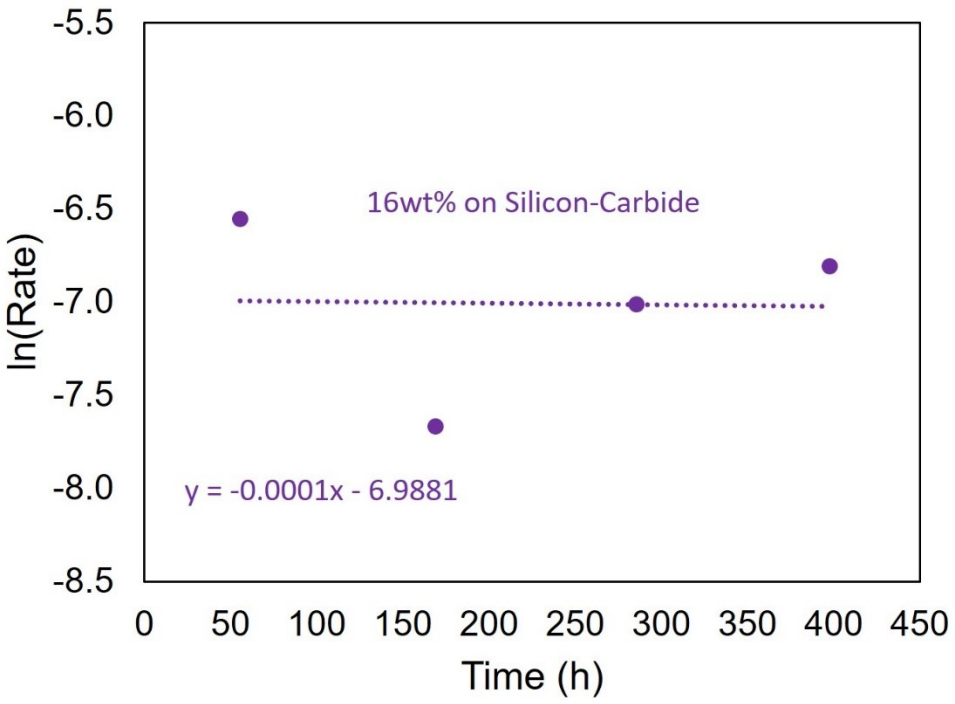

Figure S10. Catalyst stability analysis for the non-deactivating immobilized catalyst (16wt% loading of PHAH-GA-MAL-H was supported on silicon-carbide); Slope represents rate constant for catalyst deactivation ($k_{deact.}$ ~0 h^{-1}) and the averaged rates were used as a rate for lactose hydrolysis (Rate=0.0010 M·h^{-1}) and used to calculate k_{G_1H} and TOF for the active site.

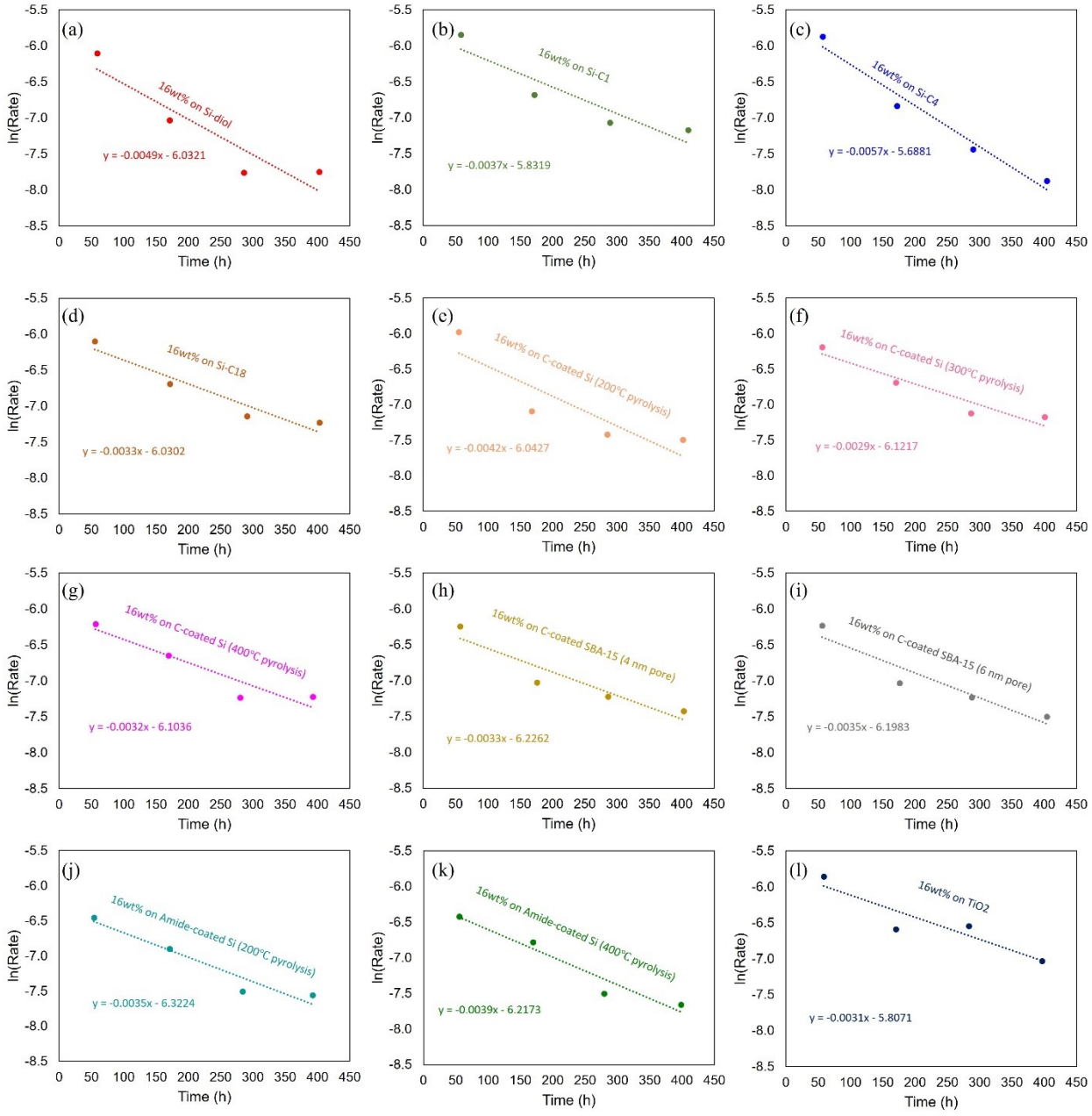

Figure S11. Catalyst stability analysis for the deactivating immobilized catalyst (16wt% loading of PHAH-GA-MAL-H) on various supports, (a) Si-diol, (b) Si-C_1, (c) Si-C_4, (d) Si-C_{18}, I C-coated Si (by pyrolysis at 200°C), (f) C-coated Si (by pyrolysis at 300°C), (g) C-coated Si (by pyrolysis at 400°C), (h) C-coated SBA-15 with 4 nm pores (by pyrolysis at 400°C), (i) C-coated SBA-15 with 6 nm pores (by pyrolysis at 400°C), (j) Acetamide-coated Si (by pyrolysis at 200°C), (k) Acetamide-coated Si (by pyrolysis at 400°C), (i) TiO_2; Slope represents the rate constant for catalyst deactivation ($k_{deact.}$), y-intercept shows the log-scale initial rate for lactose hydrolysis (ln($Rate_0$) and $Rate_0$ was used to calculate k_{G_1H} and TOF for the active site.

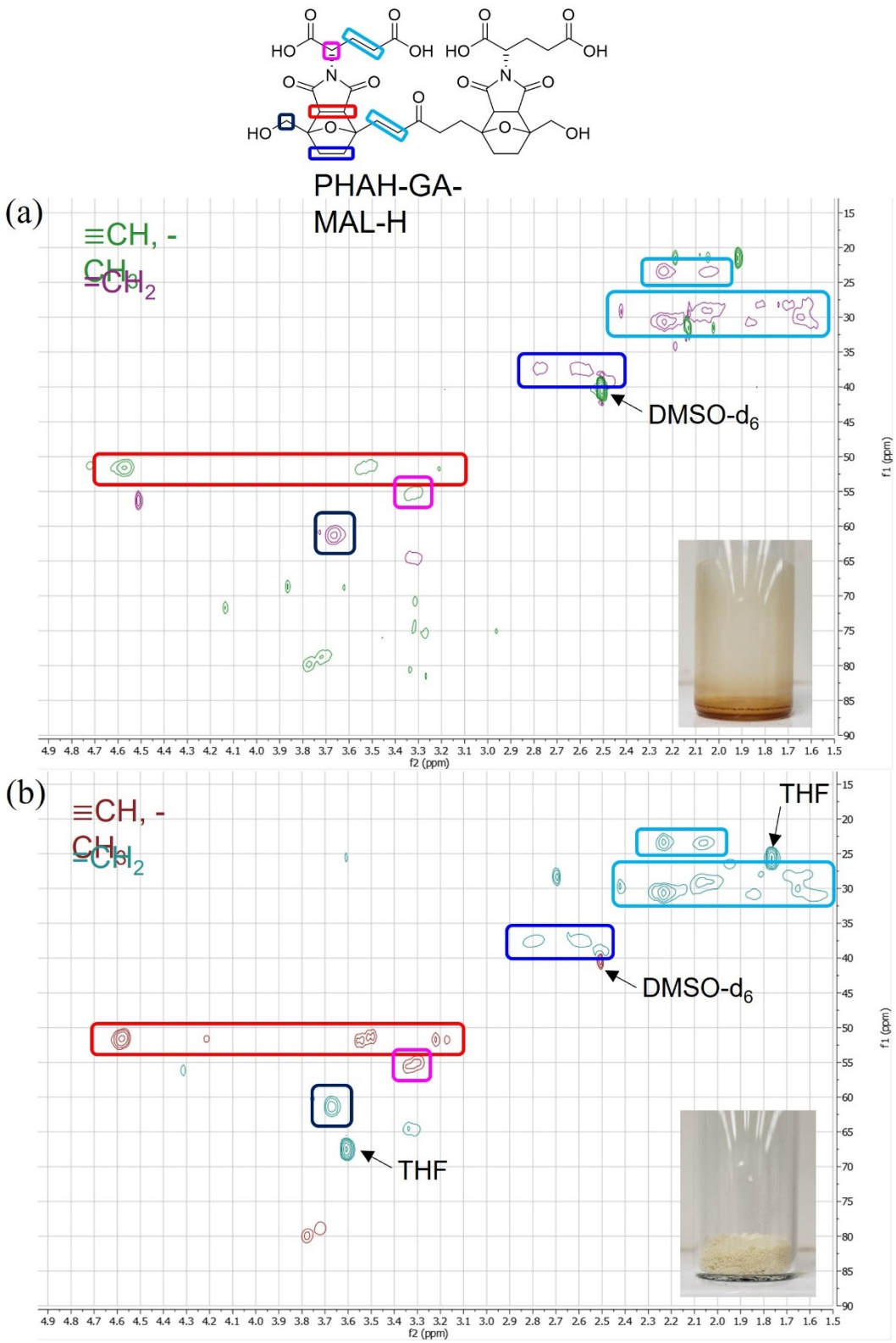

Figure S12. Comparison of 2D HSQC NMR spectrums for (a) the extracted PHAH-GA-MAL-H from Si-C_4 support after 5th cycle of lactose hydrolysis and (b) Fresh PHAH-GA-MAL-H (Deuterated solvent: DMSO-d_6).

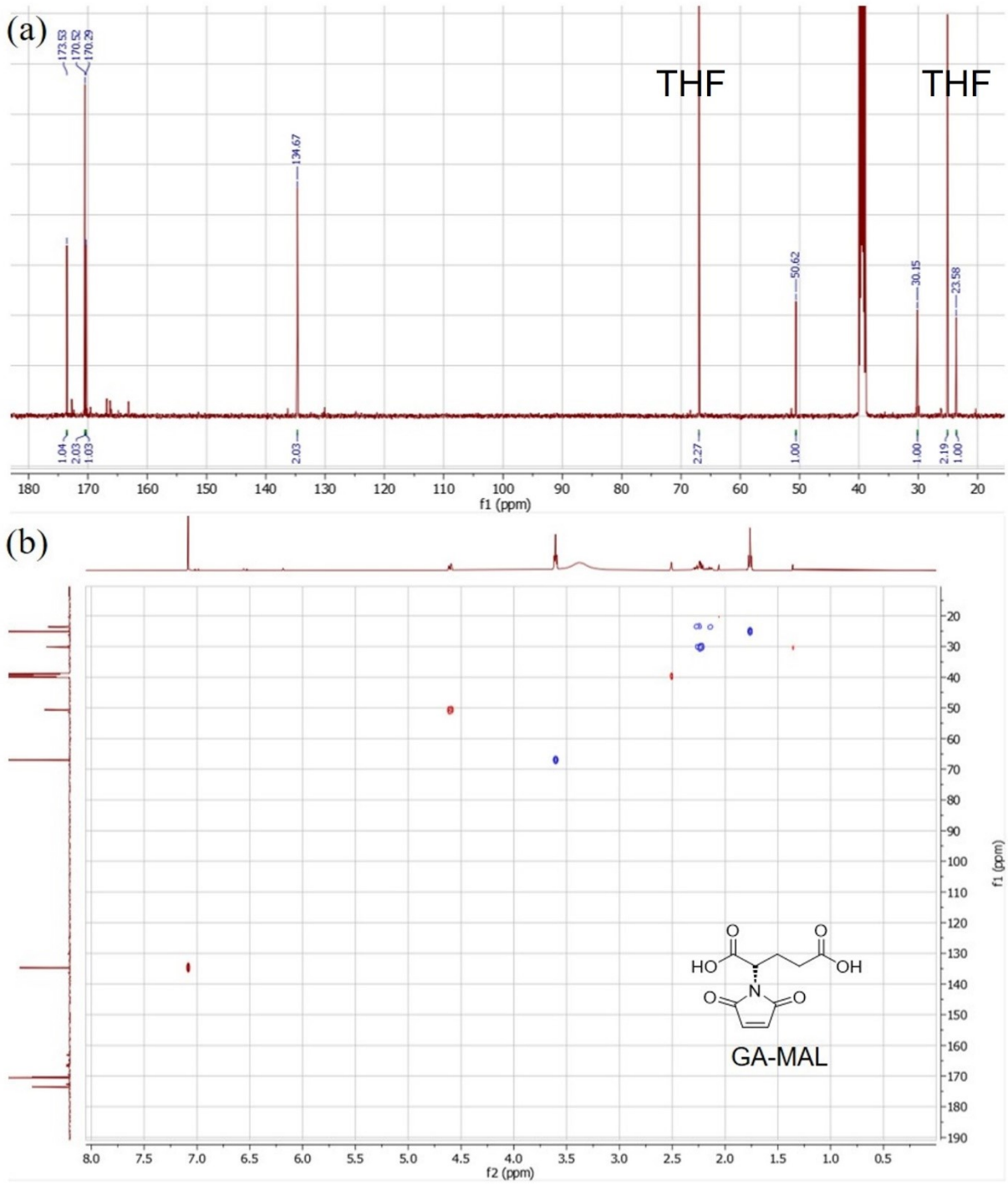

Figure S13. Characterization of GA-MAL by (a) ^{13}C qNMR (Chemical shift, δ: 172.53 (C1), 170.52 (C2), 170.29 (C1), 134.67 (C2), 50.62 (C1), 30.15 (C1), 23.58 (C1) ppm) and (b) 2D HSQC NMR spectrum (Red dot: $-CH_3$ and ≡CH group, Blue dot: $=CH_2$ group, Deuterated solvent: DMSO-d_6).

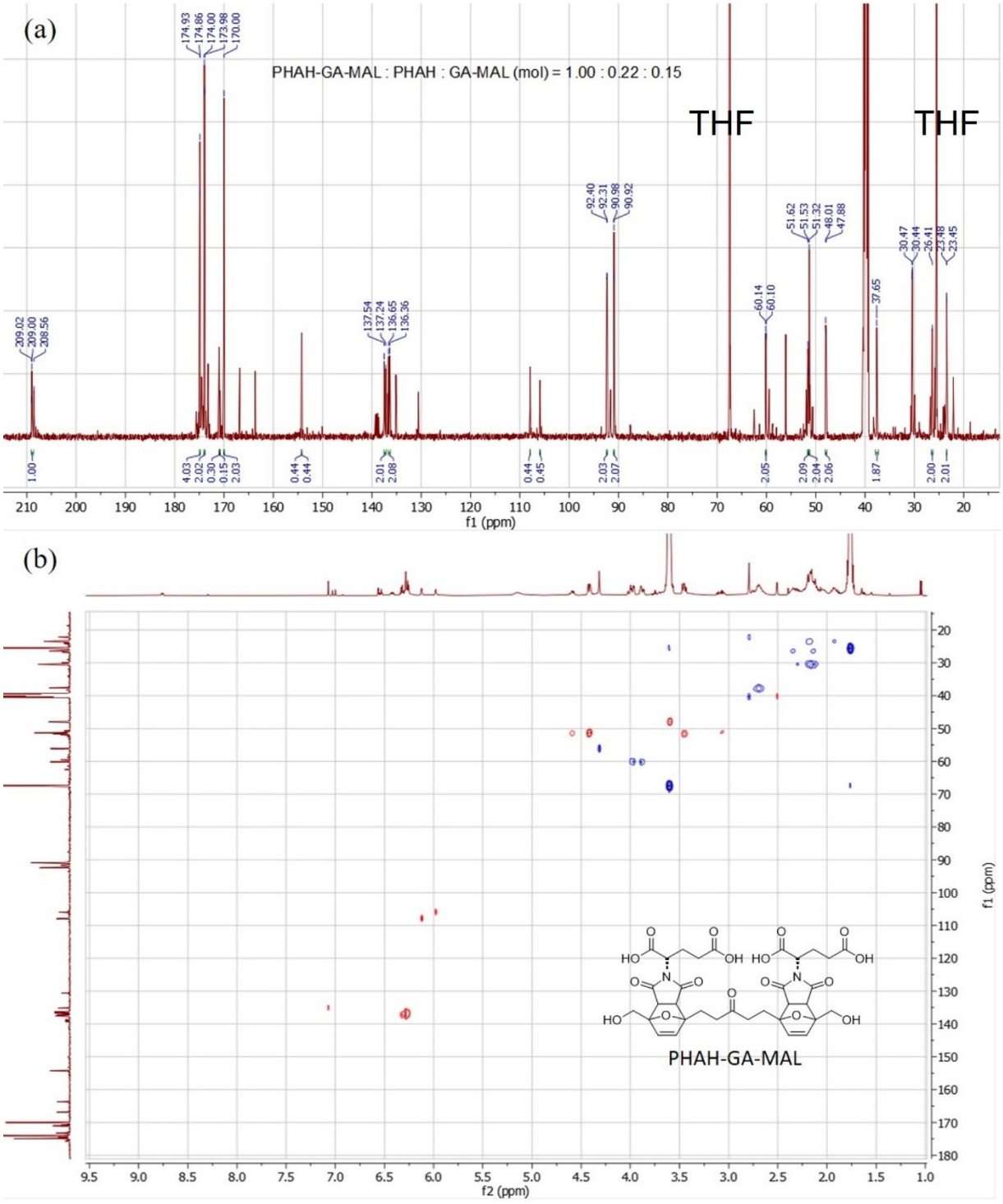

Figure S14. Characterization of PHAH-GA-MAL by (a) ^{13}C qNMR (Chemical shift, δ: 209.02-208.56 (C1), 174.93 (C4), 174.86 (C2), 170.00 (C2), 137.54-137.24 (C2), 136.65-136.36 (C2), 92.40-92.31 (C2), 90.98-90.92 (C2), 60.14-60.10 (C2), 51.62-51.32 (C4), 48.01-47.88 (C2), 37.65 (C2), 30.47-30.44 (C2), 26.41 (C2), 23.48-23.45 (C2) ppm) and (b) 2D HSQC NMR spectrum (Red dot: -CH_3 and ≡CH group, Blue dot: =CH_2 group, Deuterated solvent: DMSO-d_6).

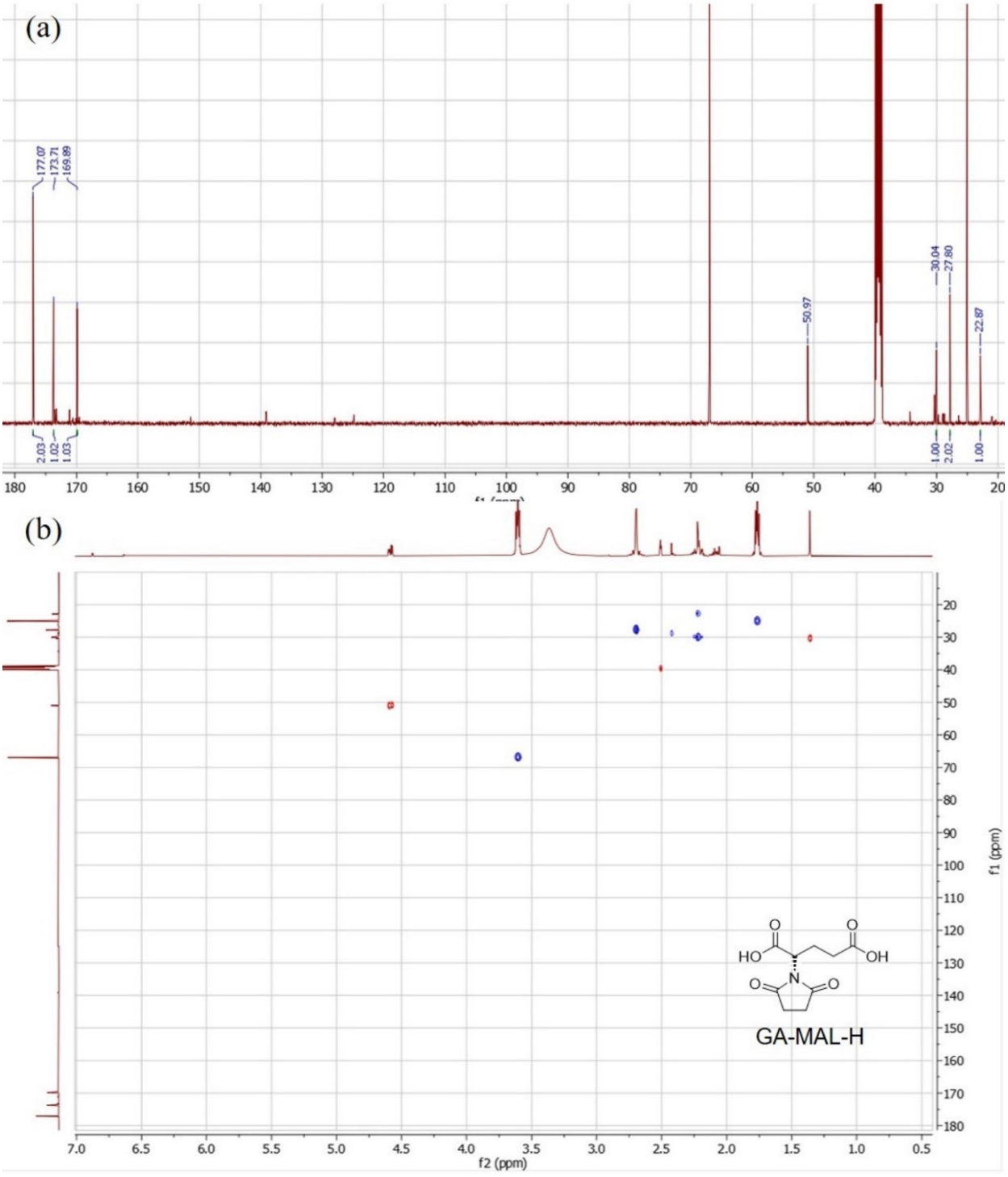

Figure S15. Characterization of GA-MAL-H by (a) ^{13}C qNMR (Chemical shift, δ: 177.07 (C2), 173.71 (C1), 169.89 (C1), 50.97 (C1), 30.04 (C1), 27.80 (C2), 22.87 (C1) ppm) and (b) 2D HSQC NMR spectrum (Red dot: $-CH_3$ and ≡CH group, Blue dot: $=CH_2$ group, Deuterated solvent: DMSO-d_6).

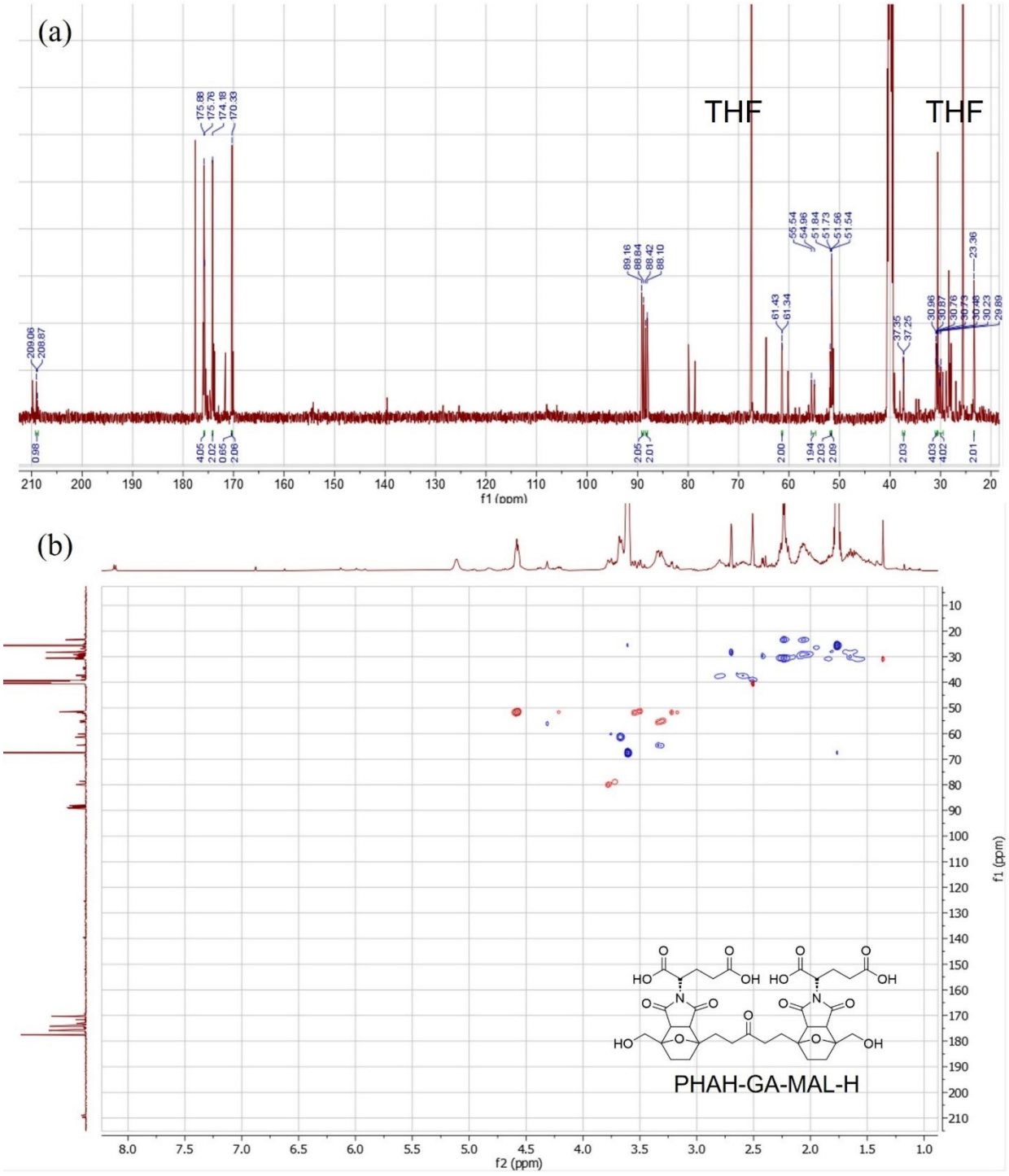

Figure S16. Characterization of PHAH-GA-MAL-H by (a) ^{13}C qNMR (Chemical shift, δ: 209.06-208.87 (C1), 175.88 (C4), 175.76 (C2), 170.33 (C2), 89.16-88.84 (C2), 88.42-88.10 (C2), 61.43-61.34 (C2), 55.54-54.96 (C2), 51.84-51.73 (C2), 51.56-51.54 (C2), 37.35-37.25 (C2), 30.98-30.76 (C4), 30.73-29.89 (C4), 23.36 (C2) ppm) and (b) 2D HSQC NMR spectrum (Red dot: $-CH_3$ and ≡CH group, Blue dot: $=CH_2$ group, Deuterated solvent: DMSO-d_6).

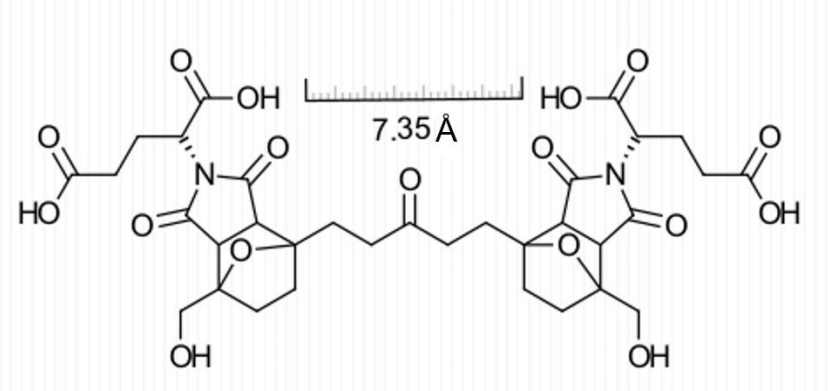

Figure S17. Measurement of physical distance between two active sites (G_1H, α-carboxylic acid) in PHAH-GA-MAL-H (by ChemDoodle software).